engineering proceedings

Proceeding Paper

Initial Experimentation of a Real-Time 5G mmWave Downlink Positioning Testbed †

José A. del Peral-Rosado [1,*], Ali Y. Yildirim [1], Auryn Soderini [1], Rakesh Mundlamuri [2], Florian Kaltenberger [2], Elizaveta Rastorgueva-Foi [3], Jukka Talvitie [3], Ivan Lapin [4] and Detlef Flachs [1]

1 Airbus Defence and Space, Taufkirchen, Germany
2 Eurecom, Sophia-Antipolis, France
3 Tampere University, Tampere, Finland
4 European Space Agency, Noordwijk, The Netherlands
* Correspondence: Jose_Antonio.del_Peral_Rosado@airbus.com
† Presented at European Navigation Conference, Noordwijk, 22-24 May 2024.

Abstract: This work presents the initial experimentation of a real-time 5G mmWave downlink positioning testbed deployed at Airbus premises. This experimentation is part of a first-of-a-kind testbed for hybrid Global Navigation Satellite Systems (GNSS), 5th Generation (5G) new radio (NR) and sensor positioning, called Hybrid Overlay Positioning with 5G and GNSS (HOP-5G) testbed. The mmWave 5G base station (BS) exploits the 5G standard positioning reference signal (PRS) to support positioning capabilities within the 5G NR downlink transmissions. Outdoor field results are used to characterize the received power levels and beam-based angle-of-arrival (AoA) estimation accuracy of this 5G mmWave PRS platform. The goal is to assess the suitability of this platform to enhance the positioning performance thanks to the 5G downlink mmWave transmissions. To the best of authors knowledge, this paper presents the first AoA results using OpenAirInterface (OAI) PRS mmWave signal transmissions at 27GHz for positioning. These initial field results indicate a maximum coverage of 30m and the AoA accuracy limited by the reduced array size. The limitations and potential enhancements of this platform are provided as future recommendations.

Keywords: 5G positioning; mmWave; FR2; Real-time Testbed

Citation: To be added by editorial staff during production.

Academic Editor: Firstname Lastname

Published: date

1. Introduction

Millimeter-wave (mmWave) communications at carrier frequencies above 24 GHz are one the disruptive technologies in 5th Generation (5G) new radio (NR) systems, thanks to the large bandwidth available in those high frequency bands. In addition, the large path loss suffered at mmWave bands leads to the use of directional antennas or beamforming techniques together with a high network density, offering angle-of-arrival (AoA) capabilities under line-of-sight (LoS) conditions. As a result, these broadband transmissions with beamforming capabilities in favorable propagation conditions offer also a key disruptive feature for 5G precise positioning targeting sub-meter level accuracies [1, 2], as well as for 6th Generation (6G) localization and sensing use cases [3].

Dedicated 5G network features for positioning purposes are already specified in the 3GPP NR standard, such as the 5G-based positioning methods in [4], the NR positioning reference signal (PRS) in [5], and the NR positioning protocol A (NRPPa) in [6]. Indeed, the achievable positioning capabilities of 5G-based positioning and its enhancements, such as with downlink time-difference of arrival (DL-TDoA), have been evaluated in the 3GPP standardization since Release 16 in [7], through simulations for frequency range 1 (FR1) below 6 GHz and for FR2 above 24 GHz. However, the real-world demonstration of 5G precise positioning has been very limited, due to major challenges when developing a real-time 5G network able to exploit high bandwidths required for precise positioning. For instance, a FR1 field trial of 5G positioning based on single- and multi-cell round-trip time (RTT) and uplink angle-of-arrival (AoA) is demonstrated in [8] to achieve meter-level accuracies in FR1 LoS conditions. Another relevant example is the Hybrid Overlay Positioning with 5G and GNSS (HOP-5G) testbed [9-12], where the world's first airborne 5G network for positioning purposes is shown to enable sub-meter localization accuracy with 80-MHz downlink PRS in FR1 LoS. In terms of prototype 5G FR2 network deployments, 5G mmWave precise positioning is demonstrated to achieve meter-level accuracies with downlink angle-of-departure (AoD) positioning in [13], or sub-meter-level accuracies with DL-TDoA in [14], depending on the network synchronization. Nonetheless, there is a very limited literature on 5G mmWave network deployments for precise positioning in outdoor environments.

There are certainly extensive efforts in the literature to develop high-end mmWave testbeds able to exploit the most advanced 5G FR2 and future 6G communication features. The state-of-the-art of mmWave front ends and testbeds at 28 GHz and 60 GHz is summarized in [15], including an overview of the example COSMOS testbed able to operate in both mmWave bands. Recently, an end-to-end connection between OpenAirInterface (OAI) FR2 network and a commercial UE has been demonstrated in [16]. High-end mmWave front ends with 64-element antenna array for a single 5G transmitter and 256-element array for a single 5G receiver are deployed in [17], over a controlled indoor LoS environment to achieve centimeter-level ToA accuracy. Field results with a 5G mmWave base station and a prototype UE with 16-element array are shown in [18], to assess experimental RTT, downlink AoD and uplink AoD positioning for vehicular applications.

This work is a continuation of the FR1 positioning contributions within the HOP-5G testbed in [9-12]. In contrast to prototype commercial network demonstrators, the HOP-5G testbed is an experimental and flexible proof-of-concept (PoC) of advanced 5G and hybrid positioning features, based on OAI open-source software, commercial-of-the-shelf (COTS) computing and software-defined radio (SDR) equipment, as well as custom-built payload platforms for unmanned aerial vehicles (UAV) or drones in aerial networks. In this paper, a 16-element mmWave front end at both transmitter and receiver is presented to assess the real-time beam-based AoA performance with downlink 5G PRS transmissions. To the best of authors knowledge, this is the first work on a real-time 5G mmWave PRS testbed with limited front ends assessing the downlink AoA performance outdoors.

2. OAI-based 5G mmWave Network

The OAI is an open-source software that implements a full 5G protocol and is widely used in research and experimental testbeds [19]. During recent years, OAI has also introduced the support of positioning capabilities, with key developments originated from the HOP-5G project. The physical layer includes the sounding reference signals (SRS) as in 3GPP Release 15 and the PRS as in 3GPP Release 16, both necessary to perform UL- and DL-based positioning methods, respectively. Moreover, OAI has implemented the NRPPa protocols and procedures to perform standard-compliant UL-TDoA positioning [20], where a development of the Location Management Function (LMF) also exists.

There are several examples on the use of OAI for positioning, in addition to HOP-5G testbed. In [21], OAI is combined with a multi-channel SDR and a custom 2x2 patch antenna array for enhanced cell-ID (E-CID) positioning in indoor scenarios, by using RTT and AoA estimates based on the demodulation reference signal (DM-RS). Thanks to the OAI PRS developments in the HOP-5G project, a testbed with four OAI base stations or gNBs and the OAI user equipment is deployed in [22] to exploit the PRS transmissions for DL-TDoA positioning. More recently, a novel framework is presented in [23] to estimate the RTT between a UE and a gNB with existing 5G NR transmissions.

In this paper, the OAI-based 5G mmWave network is based on downlink PRS transmissions between a single gNB and a single UE to estimate the time-of-arrival (ToA) and the received signal reference power (RSRP) at the OAI UE. The following subsections further describe the ToA and RSRP estimators.

2.1. Positioning Reference Signal

The 5G NR PRS is specified in the 3GPP standard since Release 16 as a reference signal dedicated for positioning purposes, with enhancements introduced as of the current standard in [5]. The PRS can be flexibly configured to adapt to the positioning application, by using tailored configurations of the PRS sequence and its resource allocation, such as based on the number of consecutive orthogonal frequency-division multiplexing (OFDM) symbols per slot, bandwidth or beams. In OAI, the PRS is explicitly implemented for 30 kHz and 120 kHz subcarrier spacing, corresponding to numerology 1 and 3, respectively. Furthermore, the implementation of PRS in OAI also supports the flexible resource allocation in terms of frequency, time and beams.

The resource allocation of the PRS implementation in OAI mmWave configuration is here defined by a subcarrier spacing of 120 kHz, 64 physical resource blocks (PRBs) occupying a bandwidth of 92.16 MHz, 6 consecutive OFDM symbols, comb-size of 4 (i.e., one every four subcarriers used for PRS resource elements), and allocated for 8 different beams. The resulting PRS resource allocation within the 5G NR radioframe and within every PRS slot is shown in Figure 2.

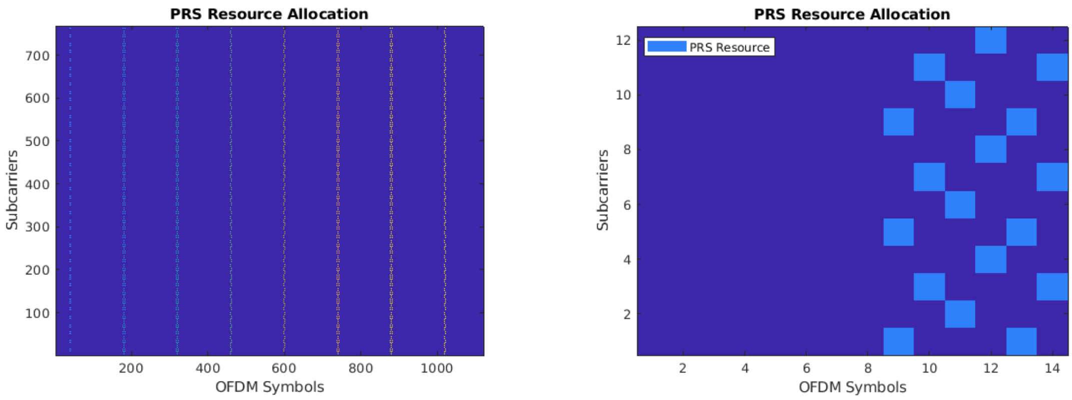

(**a**) PRS over radioframe (**b**) PRS over slot

Figure 2. OAI mmWave PRS resource allocation within: (**a**) 5G NR radioframe; (**b**) 5G NR slot.

2.2. Time-of-Arrival and Power Measurements

The ToA estimation is here based on a threshold-based correlation of the PRS, i.e., ToA for the maximum peak of the PRS correlation above a certain threshold. This is implemented with a least-squares channel estimate in the frequency domain from the PRS, which is then converted to the time domain using an Inverse Discrete Fourier Transform (IDFT) to determine the ToA.

The least-squares estimate of the PRS channel $h[k]$ at the k-th subcarrier can be obtained from the frequency-domain received signal $y[k]$ as

$$h[k] = y[k] \cdot s^*[k], \tag{1}$$

where $k \in [0, K-1]$ and K is the total number of subcarriers per PRS symbol. The frequency domain channel estimates can be represented in a vector form as,

$$\boldsymbol{h} = [h[0], h[1], \dots, h[K-1]] \in \mathbb{C}^{K\times 1}. \tag{2}$$

Then, $\boldsymbol{h}$ is zero padded by an up-sampling factor K_n represented as $\boldsymbol{h}_\mathrm{ZP} \in \mathbb{C}^{K_\mathrm{n}\cdot K\times 1}$ to increase the time resolution when converted to the time domain. The ToA estimate from $\boldsymbol{h}_\mathrm{ZP}$ is finally obtained by taking an IDFT of size $K \cdot K_\mathrm{n}$ as

$$\hat{\tau} = \frac{1}{F_s \cdot K_n} \cdot \text{argmax IDFT}\{\boldsymbol{h}_{\text{ZP}}\}, \tag{3}$$

where F_s is the sampling rate.

The RSRP in digital domain (measured in dBFS) is estimated from the received signal $y[k]$ (which is in Q1.15 fixed point format) as follows,

$$\text{RSRP[dBFS]} = 10 \cdot \log_{10}\left(\frac{1}{K}\sum_{k=0}^{K-1}|y[k]|^2\right) - 10 \cdot \log_{10} 2^{30}, \tag{4}$$

where $|\cdot|$ denotes a modulus of a complex number and 2^{30} corresponds to the power level at full scale of 30 bits. Further, to convert RSRP from dBFS to dBm, the RSRP in dBm is obtained by

$$\text{RSRP[dBm]} = \text{RSRP[dBFS]} - G_{\text{RX}}, \tag{5}$$

where G_{RX} is the receiver gain, which is calibrated using a signal at a known input level.

3. Beam-based Angle-of-Arrival Algorithm

The AoA estimation is here performed with a beam-based AoA algorithm. First, the the mmWave front end at the receiver scans a certain angle estimation range by sweeping the pre-selected analogue beams from the beambook. Then, the AoA is estimated by weighting the receive power measurements of each analogue beam scanned.

A polynomial fitted to the RSRP measurements of the PRS allows to interpolate the signal strength between the receive beams and estimate the AoA of the signal with accuracy exceeding the beam separation. Let us assume that the UE receives the PRS signal via M receive beams, with beam directions in the azimuth angle domain $\boldsymbol{\phi} \in \mathbb{R}^M$ spanning the desired AoA estimation range that includes the (unknown) AoA of the LoS path, ϕ_{AoA}. Let us also assume that the signal received via each receive beam is in a form of raw I/Q samples, with I and Q signals output recorded simultaneously through the separate output ports to obtain the baseband real part and imaginary part of the receive signal, respectively. Assuming appropriate signal synchronization and cyclic prefix (CP) removal, the output of these two ports can be combined into a vector of complex samples as $\boldsymbol{S}_{\text{RX}} \in \mathbb{C}^N$, where N is the number of OFDM symbol samples. Each beam-based RSRP measurement, therefore, can be obtained as

$$P_{\text{b}} = 10 \cdot \log_{10}\left(\frac{\sum_{i\in\Omega}|\boldsymbol{X}_{\text{RX},i}|^2}{K}\right) \in \mathbb{R}, \tag{6}$$

where $\boldsymbol{X}_{\text{RX},i}$ denotes the discrete Fourier transform of $\boldsymbol{S}_{\text{RX}}$, and Ω denotes the set of PRS active subcarrier indices of cardinality K. The RSRP measurements for all RX beams can be represented as a function of the beam azimuth angle $\mathbf{P}_b(\boldsymbol{\phi}) \in \mathbb{R}^M$, corresponding to the horizontal RSRP profile of the received signal.

The proposed AoA estimation algorithm is then built upon a polynomial fitting of the RSRP profile using the weighted least squares (WLS) method. In particular, the vector $\mathbf{P}_b$ is approximated with the second-degree polynomial (parabola) $\widetilde{\boldsymbol{P}_b} = c_0 + c_1\phi + c_2\phi^2$ subject to a Gaussian weighting function $w(\phi) = e^{-\frac{1}{2}\left(\frac{\phi-\phi_{\max}}{\sigma}\right)^2}$, which is centered around the beam azimuth with the largest power $\phi_{\max} = \text{argmax}(\boldsymbol{P}_b)$ and standard deviation σ, being a user-defined parameter. The AoA estimate can be calculated in closed form as a function of the polynomial coefficients:

$$\hat{\phi}_{\text{AoA}} = -c_1/(2c_2). \tag{6}$$

In case the RSRP measurements suffer from errors due to very low SNR or interference, or in case the amount of receive beams is not enough to define the maximum of $\mathbf{P}_b$, the parabola may be inverted or degenerate, which does not allow to estimate ϕ_{AoA}. A condition $c_2 < 0$ ensures that this does not happen, and AoA can be estimated using Equation (6). Note that in case this condition does not hold and parabolic approximation does not exist, AoA can be estimated as a direction of the beam with highest RSRP measurement, i.e., $\hat{\phi}_{\mathrm{AoA}} = \phi_{\max}$.

An example result of the AoA beam-based algorithm is shown in Figure 3.

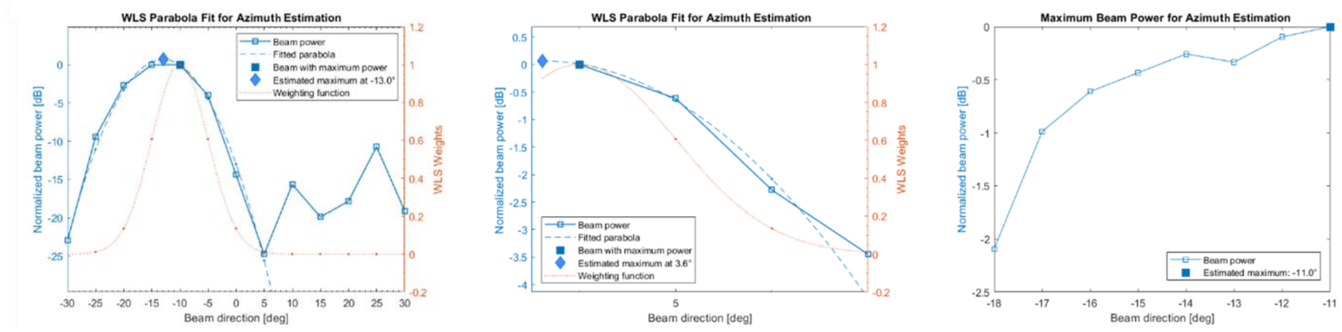

(**a**) (**b**) (**c**)

Figure 3. Example of beam-based AoA estimation demonstrated on test data obtained with horn antenna as a transmitter and beam-sweeping Anokiwave antenna array with a fixed gain as a receiver: (**a**) maximum power is defined, parabola fit is successful, and AoA is estimated as interpolation between beam directions; (**b**) parabola fit is successful, and AoA is estimated as extrapolation beyond the range of azimuth angle ϕ; (**c**) maximum is on the boundary, parabola fit is unsuccessful, and AoA is estimated as a direction of a beam with maximum power value. Note that beam powers are normalized to the maximum value. This test setup does not use any SDR.

Note that the above beam-based AoA algorithm is presented for the azimuth beamforming at the UE. However, in case of elevation beamforming, the same principle can be applied to the elevation or zenith angle θ_{AoA} using the vertical RSRP profile, or extended to fitting a parabolic surface in case of tridimensional (3D) beams.

4. HOP-5G mmWave Positioning Testbed

The HOP-5G mmWave positioning testbed is based on a fixed mmWave gNB and moving mmWave UE, as it is shown in Figure 4. This testbed follows a modular architecture to enable the operation of each node as transmitter or receiver with specific hardware and software configurations. The key hardware components of the testbed are:

- mmWave front end: The Sivers EVK02001 is an analogue beamformer mmWave front end (FE) able to up-convert from baseband to mmWave or to down-convert from mmWave to baseband the 5G NR signals. The 16-element antenna array, i.e., uniform rectangular array (URA) with 2 x 8 elements, enables steerable beams within the beambook upon operator commands.
- Software-defined radio: The USRP X310 is a flexible SDR, which here includes a BasicTX or BasicRX daughterboard for transmission or for reception, respectively, and a GPS disciplined oscillator (GPSDO) to increase the stability of the SDR clock. This SDR is used to stream the baseband samples of the 5G NR signals between the mmWave front end and the host computer.
- Host computer: The host computer includes the necessary software modules to establish the 5G transmission, 5G reception, GNSS data collection and AoA estimation. At the transmission, the OAI gNB is used to stream the 5G PRS to the mmWave front end through the SDR in real-time. At the reception, the OAI UE is used to process the 5G PRS and to obtain ToA and RSRP measurements in real-time, and the AoA estimator controls the beams of the mmWave front end and computes the AoA measurements also in real-time. In both nodes, the GNSS receiver manager operates and collects the GNSS position solution from the receiver in real-time.

- GNSS receiver: The u-blox F9P is a multi-band high precision GNSS receiver, whose position solution is used for the ground truth of the field campaign.
- GNSS antenna: A survey multi-band GNSS antenna is used at both nodes together with a splitter to feed GNSS signals to the USRP GPSDO and to the GNSS receiver.

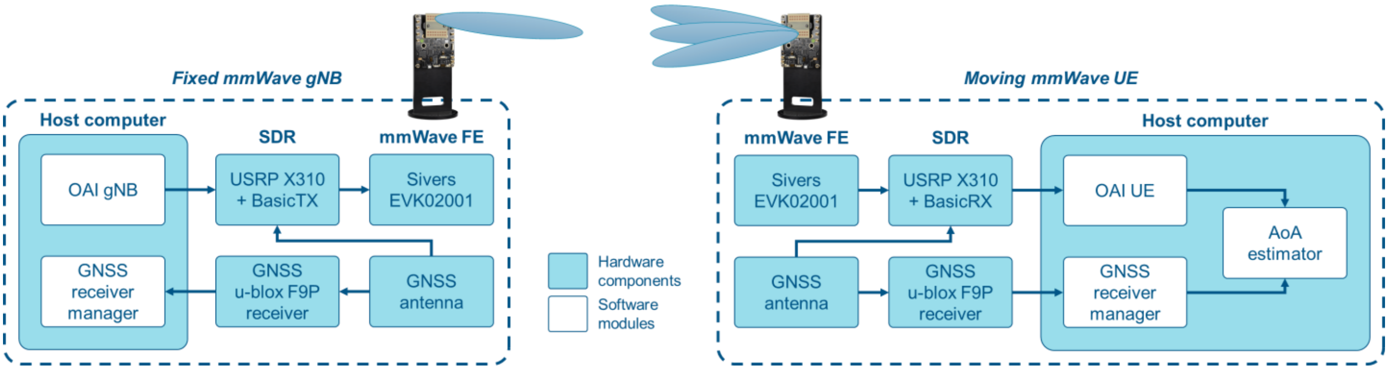

Figure 4. Architecture of the HOP-5G mmWave positioning testbed.

The AoA estimation software module at the UE host computer controls the mmWave front end to enable the real-time AoA measurements. This module connects to the Sivers EVK and initiates its operation. Then, the software proceeds to establish the reception beam on the antenna array. As it is described in Sec. 3, the beam-based AoA estimation is performed with the RSRP measurements of the PRS received from the gNB for each beam. Thus, the AoA algorithm collects RSRP measurements for each beam angle, and proceeds to sweep each beam within -45 degree to 45 degree with a 4.5-degree resolution per beam. The reception duration for each beam angle is of 20ms, which is sufficient for OAI UE to perform and disseminate the PRS RSRP and ToA measurements. The measurement dissemination is performed over the MQTT protocol. The OAI publishes the measurements messages in a specific MQTT topic, and the AoA algorithm subscribes to this topic to collect the measured RSRP measurements for each reception beam angle. Since the RSRP collection lasts 20ms for each beam, the overall measurement collection has a duration of 420ms for all beams. After the RSRP collection, the AoA algorithm estimates the reception angle in real-time. The AoA algorithm also collects the most recent position solution published by the GNSS receiver manager over MQTT. Finally, the AoA algorithm outputs the AoA estimation together with the RSRP measurements and GNSS position solution.

5. Field Campaign

This section discusses the initial experimentation results on the maximum coverage distance and receiver orientation impact, when using the HOP-5G mmWave positioning testbed in a field campaign.

5.1. Description

HOP-5G mmWave positioning testbed is deployed on demand at Airbus premises for experimentation purposes. The FR2 downlink transmission is established at 27 GHz with a static OAI gNB and a moving OAI UE. The 5G PRS configuration described in Sec. 2.1 is used to achieve a bandwidth of 92.16 MHz. As it is shown in Figure 5, the starting position of the UE is as close as possible to the gNB, and then the UE (mounted on a trolley) is moved linearly until a maximum coverage distance. The UE moves with a nearly linear trajectory at a nearly constant and low velocity, i.e., with variations between 0.25m/s and 1 m/s, except at planned temporary stops to evaluate the static scenario.

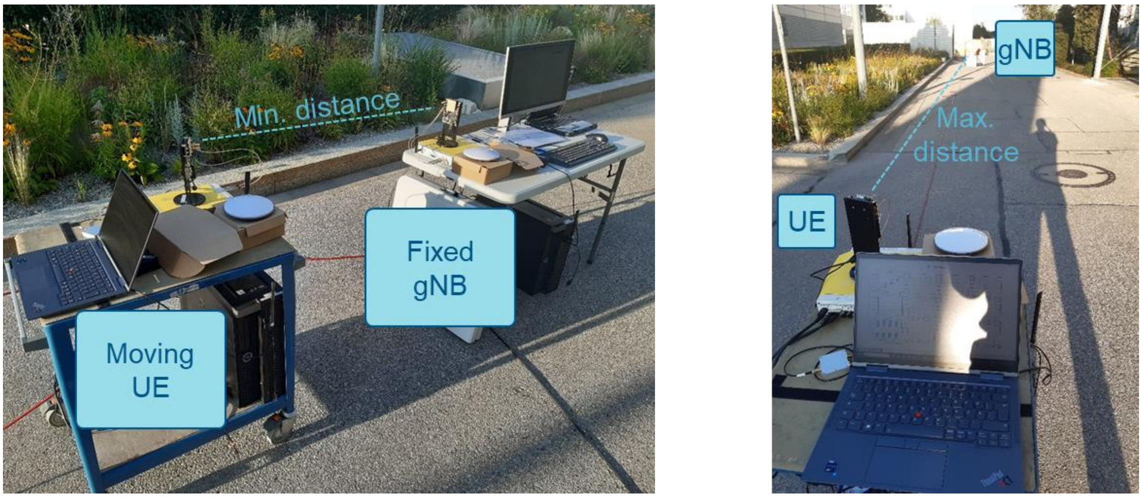

(**a**) (**b**)

Figure 5. Field deployment of the HOP-5G mmWave positioning testbed: (**a**) Tests start at minimum distance between gNB and UE; (**b**) Tests finalize at maximum coverage between gNB and UE.

The field experimentation is based on a five-step procedure repeated in each test to perform the AoA measurements:

1. The OAI UE acquires and tracks the 5G NR signals transmitted from OAI gNB;
2. The GNSS receiver manager collects and disseminates in real-time the GNSS-based UE position solution;
3. For each beam within [-45°, -41.5°, …, 41.5°, 45°], the AoA algorithm enables the corresponding beam on the Sivers EVK, the OAI UE estimates the RSRP from the PRS subframes, and the AoA algorithm collects the RSRP measurement for the specific beam;
4. The AoA algorithm performs in real-time AoA estimation from the collected RSRPs;
5. The AoA estimate is disseminated together with the latest GNSS position solution.

The data measurements with AoA, RSRP and GNSS solution are logged in real-time and post-processed for the performance analysis.

5.2. Maximum Coverage Distance

The assessment of the maximum coverage distance is performed based on the availability of OAI measurements as the UE moves farther from the gNB. The distance between gNB and UE is computed with the stand-alone GNSS solution estimated at both nodes during the entire duration of the field test (i.e., 120 seconds).

The field results shown in Figure 6 indicate a maximum distance around 30m between UE and gNB with the HOP-5G mmWave positioning testbed. At 30m of distance, the OAI UE loses the 5G NR signal tracking, and the test is stopped before UE returns to the starting point for the following test. The AoA estimation accuracy is analyzed based on the RSRP distribution for each beam as function of the distance between UE and gNB, as it is shown in Figure 6.(a) and 6.(b). Considering the static periods within the trajectory, the average RSRP is computed for each beam angle. The result indicates an almost constant average RSRP value between beam angle -13.5° and 13.5°, while the rest of beam angles (outside of this range) include values 3 dB below. This beam pattern is kept over the different distances. As a result, when both transmitter and receiver are aligned, i.e., azimuth orientation of 0°, the AoA estimation accuracy is equal to 4.6° at static periods. The AoA performance degrades to 9.5° for the full trajectory, which includes dynamic and static periods. Certainly, the reduced array size limits the AoA estimation accuracy.

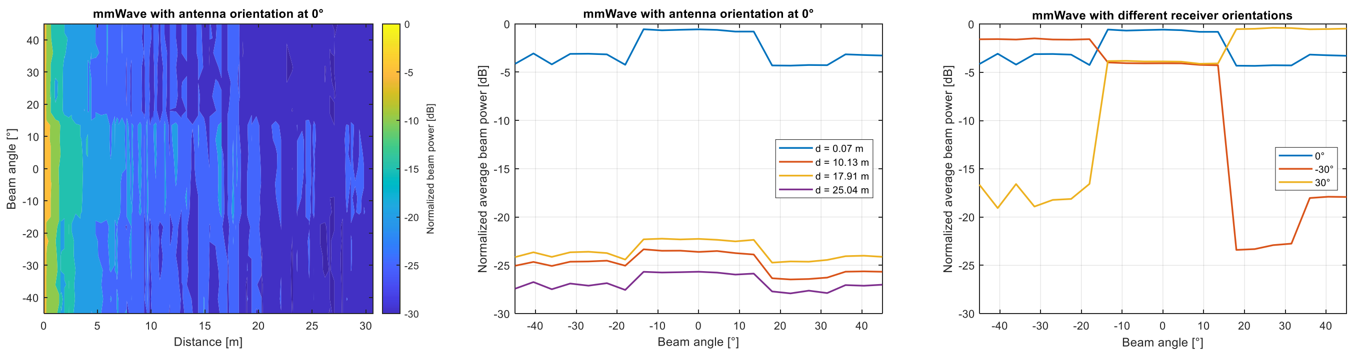

(**a**) (**b**) (**c**)

Figure 6. Power measurements per beam angle: (**a**) RSRP per beam angle over the full UE trajectory and azimuth orientation of 0°; (**b**) Average RSRP per beam angle at static UE locations within the moving trajectory and azimuth orientation of 0°; (**c**) Average RSRP per beam angle for azimuth orientation of 0°, -30°, and 30° during static UE periods.

5.2. Impact of the Receiver Orientation

The receiver azimuth orientation has also a significant impact on the beam alignment between transmitter and receiver. In order to assess this impact on the FR2 AoA estimation, several tests are repeated for different receiver orientation compared to the perfect alignment studied in the previous section, i.e., with UE orientations at 0°, 30° and -30°. The static periods of these tests are used to obtain the beam pattern for each orientation. As it is shown in Figure 6.(c), the beam pattern of the Sivers EVK is not symmetric and there are abrupt changes on the RSRP between -13.5° to -18° and between 13.5° and 18°, which correspond to angle offsets of 45° with respect to the antenna boresight. This reduces the sensitivity of the AoA to small changes in the receiver orientation, especially when perfectly aligned. Future work can explore enhanced AoA weighting functions optimized for the beam response of the antenna array or based on iterative fitting, as in [24].

6. Conclusions

This paper presents the first results of a real-time 5G mmWave testbed, able to exploit positioning reference signal (PRS) transmissions for beam-based angle-of-arrival (AoA). The testbed is based on the combination of OpenAirInterface (OAI), a software-defined radio (SDR) and a 16-element mmWave front end to be deployed at both base station (BS) and user equipment (UE) and operating at 27 GHz. The proposed beam-based AoA algorithm controls the antenna array to sweep beams over the scanned angles, while collecting receive power measurements for each beam. The initial experimentation results of the field campaign indicate a maximum distance coverage of 30 m between BS and UE. In addition, the AoA estimation is of 4.6° under UE static conditions and perfect alignment between transmitter and receiver arrays. The introduction of an orientation mismatch at UE, i.e., with azimuth orientation of -30° and 30°, results in abrupt decreases on the RSRP measurements. The beam response characterization or the iterative fitting can be used in the future to enhance the AoA performance of reduced antenna arrays.

Author Contributions: Conceptualization, J.A.d.P.R., A.Y.Y., A.S., R.M., F.K., E.R.F., J.T. and D.F.; experimentation, J.A.d.P.R., A.S.; data post-processing, J.A.d.P.R. and A.S.; writing, J.A.d.P.R, A.Y.Y., A.S., R.M., F.K., E.R.F., J.T.; project administration, J.A.d.P.R. All authors have read and agreed to the published version of the manuscript.

Funding: This work from the Hybrid Overlay Positioning with 5G and GNSS (HOP-5G) project has been supported by the European Space Agency Navigation Innovation and Support Programme (NAVISP), which aims to generate innovative concepts, technologies and system solutions in the wide-field of Positioning, Navigation and Time.

Institutional Review Board Statement: Not applicable.

Informed Consent Statement: Not applicable.

Acknowledgments: Not applicable.

Conflicts of Interest: The authors declare no conflict of interest. The view expressed herein can in no way be taken to reflect the official opinion of the European Space Agency.

References

1. del Peral-Rosado, J.A.; Raulefs, R.; López-Salcedo, J.A.; Seco-Granados, G. Survey of Cellular Mobile Radio Localization Methods: From 1G to 5G. IEEE Commun. Surveys Tuts. **2018**, 20 (2), 1124-1148.
2. Wymeersch, H.; Seco-Granados, G.; Destino, G.; Dardari, D.; Tufvesson, F.; 5G mmWave positioning for vehicular networks. IEEE Wirel. Commun. **2017**, 24 (6), 80-86.
3. Khatib, E.J.; Álvarez-Merino, C.S.; Luo-Chen, H.Q.; Barco-Moreno, R. Designing a 6G Testbed for Location: Use Cases, Challenges, Enablers and Requirements. IEEE Access **2023**, 11, 10053-10091.
4. 3GPP TS 38.305, NG Radio Access Network (NG-RAN); Stage 2 functional specification of User Equipment (UE) positioning in NG-RAN. Release 18, 2024.
5. 3GPP TS 38.211, NR; Physical channels and modulation. Release 18, 2024.
6. 3GPP TS 38.455, NG-RAN; NR Positioning Protocol A (NRPPa). Release 18, 2024.
7. 3GPP TR 38.855, Study on NR positioning support. Release 16, 2019.
8. Qualcomm, ZTE and China Mobile. 5G Multi-cell Positioning: Joint Field Trial Demonstration. Available online: https://www.qualcomm.com/videos/5g-multi-cell-positioning-ota-demonstration (accessed on 5 Sep. 2024)
9. del Peral-Rosado, J. A.; et al. Design Considerations of Dedicated and Aerial 5G Networks for Enhanced Positioning Services. *Proc. NAVITEC* **2022**, 1-12.
10. del Peral-Rosado, J. A.; et al. Proof-of-Concept of Dedicated Aerial 5G and GNSS Testbed for Enhanced Hybrid Positioning. *Proc. ION GNSS+* **2022**, 1-15.
11. del Peral-Rosado, J.A.; et al. Preliminary Field Results of a Dedicated 5G Positioning Network for Enhanced Hybrid Positioning. *Eng. Proc.* **2023**, 54 (6).
12. del Peral-Rosado, J. A.; et al. First Field Trial Results of Hybrid Positioning with Dedicated 5G Terrestrial and UAV-Based Non-Terrestrial Networks. *Proc. ION GNSS+* **2023**, 1598-1605.
13. Qualcomm. MWC 2022: Expanding 5G positioning to mmWave and lower-complexity IoT. Available online: https://www.youtube.com/watch?v=82zIWOa2PhI (accessed on 5 Sep. 2024)
14. Qualcomm. MWC 2023: Precise Positioning and RF Sensing. Available online: https://www.qualcomm.com/videos/precise-positioning-and-rf-sensing (accessed on 5 Sep. 2024)
15. Chen, T.; et al. Open-access millimeter-wave software-defined radios in the PAWR COSMOS testbed: Design, deployment, and experimentation. Comput. Netw., Oct. **2023**, 234 (109922).
16. TMYTEK. mmW-OAI Solution: Open-Source 5G FR2 Test Network. Available online: https://tmytek.com/solutions/mmW-OAI (accessed on 5 Sep. 2024)
17. Yammine, G.; et al. Experimental Investigation of 5G Positioning Performance Using a mmWave Measurement Setup. *Proc. IPIN* **2021**, 1-8.
18. Ge, Y.; et al. Experimental Validation of Single Base Station 5G mmWave Positioning: Initial Findings. *Proc. FUSION* **2022**, 1-8.
19. Kaltenberger, F.; Silva, A.P.; Gosain, A.; Wang, L.; Nguyen, T.T. OpenAirInterface: Democratizing innovation in the 5G Era. *Comput. Netw.*, July **2020**, 176 (107284).
20. Ahadi, M.; Malik, A.; Kaltenberger, F.; Thienot, C. 5G NR UL SRS TDoA Positioning by OpenAirInterface. *Proc. IPIN-WiP* **2023**.
21. Li, D.; Chu, X.; Wang, L.; Lu, Z.; Zhou, S.; Wen, X. Performance Evaluation of E-CID based Positioning on OAI 5G-NR Testbed. *Proc. ICCC* **2022**, 832-837.
22. Palamà, I. ; Bartoletti, S.; Bianchi, G.; et al. 5G positioning with software-defined radios. *Comput. Netw.*, Aug. **2023**, 250 (110595).
23. Mundlamuri, R.; Gangula, R.; Kaltenberger, F.; Knopp, R. Novel round trip time estimation in 5G NR. *Proc. IEEE Globecom Workshops* **2024**.
24. Rastorgueva-Foi, E.; et al. Millimeter-Wave Radio SLAM: End-to-End Processing Methods and Experimental Validation. *IEEE J. Sel. Areas Commun.* Sept. **2024**, 42 (9), 2550-2567.